Numerical Simulation of Pear-shaped Bead Cracking in Narrow Gap Welding †

SHIBAHARA Masakazu*, ITO Shinsuke **, SERIZAWA Hisashi* and MURAKAWA Hidekazu******

Abstract

To achieve high efficiency and cost reduction, high heat input welding such as submerged arc welding (SAW) and CO_2 arc welding using large currents are employed. However, the high heat input given to the weld may produce coarse grains in the HAZ and a reduction of toughness. To avoid these problems, narrow gap welding which is effective in reducing heat input and achieving high productivity is often employed. However, in case of narrow gap welding, the welding conditions must be carefully selected to prevent the pear-shaped bead crack.

The pear-shaped bead crack is one of the solidification cracking forms at the grain boundary during the solidification process of the weld metal. The mechanism of the crack formation has been mostly studied from the aspect of the arc welding process. The influence of mechanical factors, such as, stress and strain fields, on the formation of cracking has not yet been clarified. The object of this research is to develop a finite element method (FEM) which can predict the formation of the pear-shaped bead crack and to clarify its mechanism based on numerical simulation so that preventive measures can be proposed

KEY WORDS: (Pear-shaped Bead Cracking) (Narrow Gap Welding) (Interface Element) (Finite Element Analysis) (Penetration Shape) (Hot Cracking)

1. Introduction

As illustrated in **Fig.1**, narrow gap welding is an effective method to achieve high efficiency and productivity. It is also effective in preventing the reduction of the ductility of the joint due to its small heat input. However, it is reported that pear-shaped bead cracking can occur when the welding conditions are not correctly chosen[1,2]. The researches on the pear-shaped bead cracking are mostly conducted based on experiments. Through these studies, it is found that the cracking is of the solidification type. The form of the crack can be divided into two types, namely the crack reaches the surface and where it does not reach the surface. **Figure 2** (a) is a photo of the pear-shaped bead cracking. Fig.2 (b) is the definition of the geometrical parameters of the penetration shape. It is also found that the formation of the pear-shaped cracking is closely related to the geometrical parameters of the penetration shape, such as the ratio between the groove width W_G and the penetration depth P. When P/W_G is greater than 1.3, the pear-shaped bead crack is likely to be formed in case of conventional arc welding. In the case of the recent arc welding shown in **Fig.3**[3], in which the welding parameters can be precisely controlled, the pear-shaped bead cracking is not observed even when the aspect ratio P/W_G is greater than this limit. If narrow gap welding with large aspect ratio becomes possible without cracking, the productivity and the quality of the weld can be further improved.

To clarify the relation between welding conditions and the formation of pear-shaped cracking, a finite element method in which the interface element[5,6] is introduced is developed. The influences of various factors on the crack formation are studied through serial computations using the proposed method.

† Received on December 1, 2003

* Joint Researcher (Assistant Professor, Kanazawa Institute of Technology)
** Graduate Student
*** Associate Professor
**** Professor

Transactions of JWRI is published by Joining and Welding Research Institute of Osaka University, Ibaraki, Osaka 567-0047, Japan

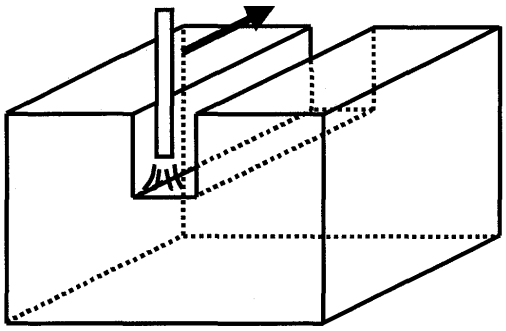

Fig.1 Schematic illustration of narrow gap welding.

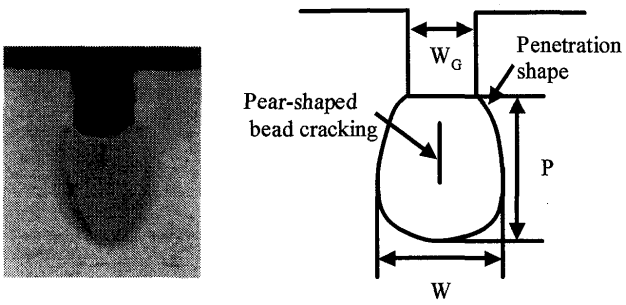

Fig.2 Photo and geometrical parameters of pear-shaped bead cracking.

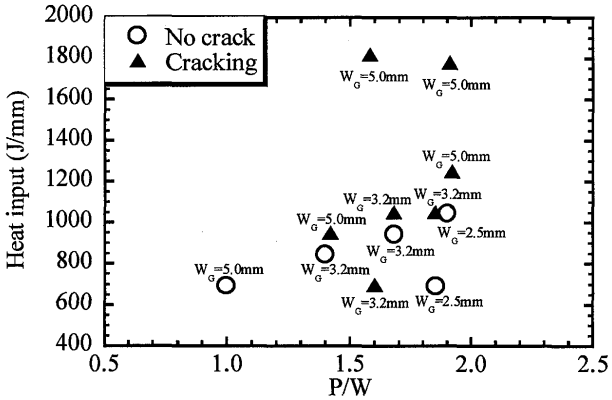

Fig.3 Effect of heat input and *P/W* on formation of pear-shaped bead cracking.

2. Theoretical formulation

2.1 Modelling of High Temperature Brittleness

Since the crack is formed when the opening stress exceeds the bonding strength of the grain boundary or the interface, the brittleness of the material at elevated temperature is modeled through the temperature dependent bonding strength of the interface element. Both the bonding strength and the yield stress are assumed to be temperature dependent. The *BTR* (Solidification Brittleness Temperature Range)[4] is modeled as the temperature range in which the bonding strength becomes smaller than the yield stress as shown in **Fig.4**. In this example, the *BTR* is between 1200 and 1450 °C. The critical strength σ_{cr} is smaller than the yield stress σ_Y in this range.

2.2 Temperature dependent interface potential

To analyze the crack formation and its extension during the welding process, a method using the interface element has been proposed[5,6]. In this method, the formation and the extension of the crack are modeled by the interface element. The mechanical behavior of the interface element is governed by the interface potential ϕ per unit area of the crack surface. The requirements of the interface potential function are

(1) It involves the surface energy γ, which is necessary to form the new surface as a material parameter.

(2) It is a continuous function of opening displacement δ.

Among many functions satisfying these requirements, a Lennard-Jones type potential γ is employed. For application to hot cracking problems, temperature dependency is introduced into the interface element through the surface energy γ. Thus, the interface potential energy γ is defined by the following equation.

$$\phi(\delta,T)=2\gamma(T)\left\{\left(\frac{r_0}{r_0+\delta}\right)^{2n}-2\left(\frac{r_0}{r_0+\delta}\right)^{n}\right\} \qquad (1)$$

where $\gamma(T)$is the surface energy per unit area which is temperature dependent. While n and r_0 are constants

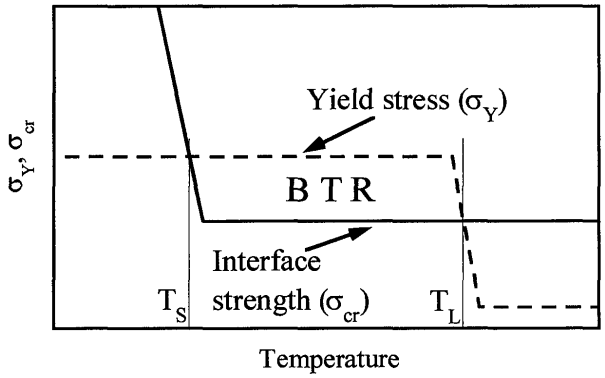

Fig.4 Temperature dependent yield stress and interface strength.

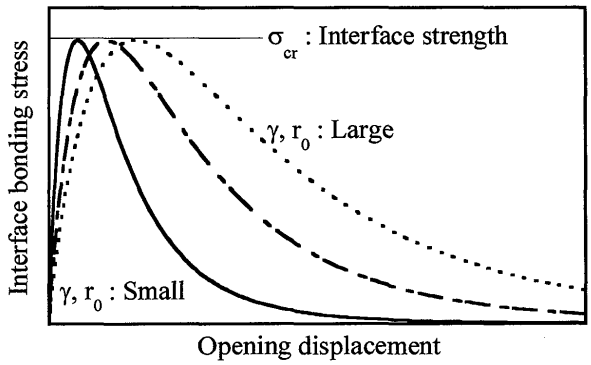

Fig.5 Stress-opening displacement curves of interface element.

independent of the temperature.

The derivative of ϕ with respect to the crack opening δ, as shown in the following equation, gives the bonding stress per unit area of the crack surface σ.

$$\sigma = \frac{\partial \phi}{\partial \delta} = \frac{4\gamma n}{r_0}\left\{\left(\frac{r_0}{r_0+\delta}\right)^{n+1} - \left(\frac{r_0}{r_0+\delta}\right)^{2n+1}\right\} \quad (2)$$

Furthermore, the bonding strength per unit area reaches a maximum value under the following condition.

$$\frac{\delta}{r_0} = \left(\frac{2n+1}{n+1}\right)^{\frac{1}{n}} - 1 \quad (3)$$

The maximum bonding strength σ_{cr} is given by

$$\sigma_{cr}(T) = \frac{4\gamma n}{r_0}\left\{\left(\frac{n+1}{2n+1}\right)^{\frac{n+1}{n}} - \left(\frac{n+1}{2n+1}\right)^{\frac{2n+1}{n}}\right\} \quad (4)$$

where σ_{cr} gives the critical strength at temperature T. Since σ_{cr} is proportional to $\gamma(T)$ as shown by Eq. (4), the temperature dependency of the surface energy γ is directly reflected in the critical strength σ_{cr}. The relation between the bonding stress σ and the opening displacement δ is presented in **Fig.5**. As is shown in the figure, the parameter r_0 is a scale parameter. When r_0 is large, the opening displacement at the formation of the crack increases. Furthermore, assuming that the surface energy is temperature dependent, the *BTR* can be modeled as shown in Fig.4. In the analysis of hot cracking, the interface elements are arranged along the path of the crack extension. Then the formation and the extension of the crack can be simulated naturally without any decision on the behavior of the crack.

3. Simulation of pear-shaped bead cracking

In this section, the proposed method is applied to narrow gap welding and the influence of various factors on the formation of the pear-shaped bead crack is investigated. The problem is treated as a two-dimensional plane strain problem. The temperature dependent interface element is arranged along the axis of symmetry in this analysis, because pear-shaped cracking occurs along the center of the weld bead. The material considered here is SM490 and its temperature dependent material properties used in the analysis are shown in **Fig.6**. The thermal expansion ratio assumed to be also temperature dependent is shown in **Fig.7**. The contraction during the solidification is considered as the thermal expansion ratio between 1300 °C and 1450 °C. The element division used for the analysis is shown in **Fig.8**. This figure shows the case in which the groove width is 5.0 mm as an example. Unless specified otherwise, the heat input is applied in 1.0 second, the groove width is 5.0 mm and the scale parameter r_0 is assumed to be 70 μm in the following computations.

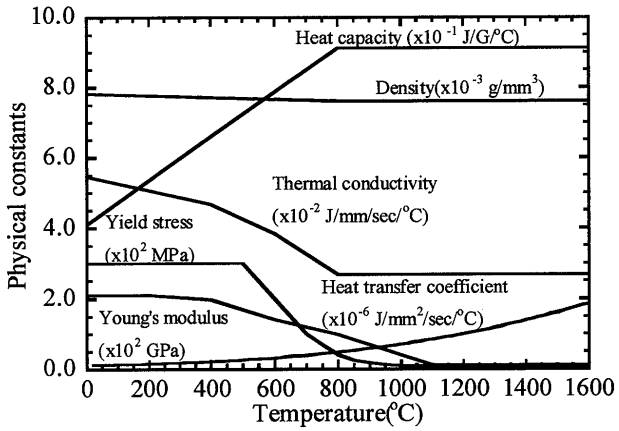

Fig.6 Temperature dependent physical constants.

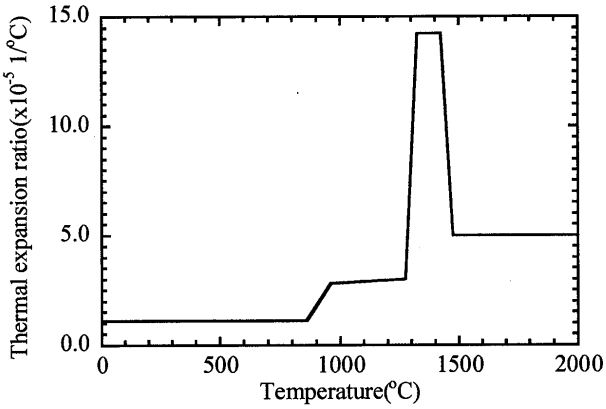

Fig.7 Temperature dependent thermal expansion ratio.

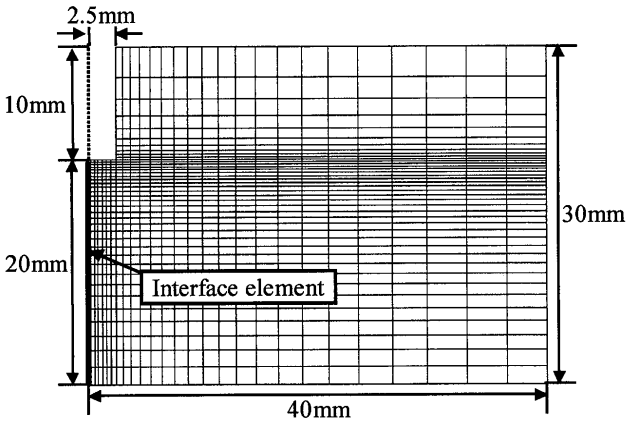

Fig.8 FEM mesh division for narrow gap welding.

3.1 Influence of heat input and *P/W*

The formation of the pear-shaped bead cracking is influenced by various factors, such as the heat input, the aspect ratio of the penetration, the welding speed, the groove width and the contraction during solidification. In this section, the influence of the heat input and the aspect ratio of penetration is investigated through serial computations changing these parameters. **Figure 9**

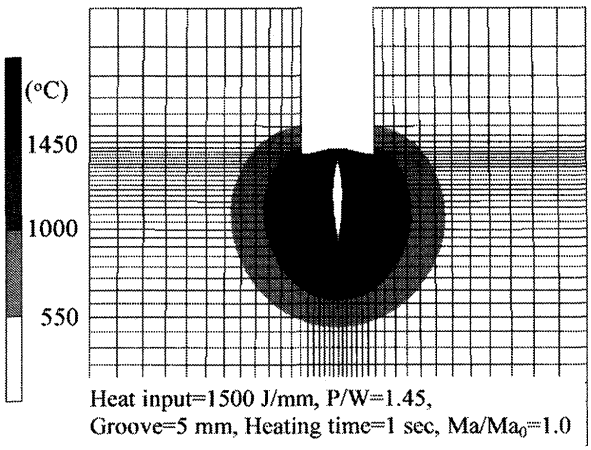

Fig.9 Maximum temperature distribution and deformation with pear-shaped bead cracking.

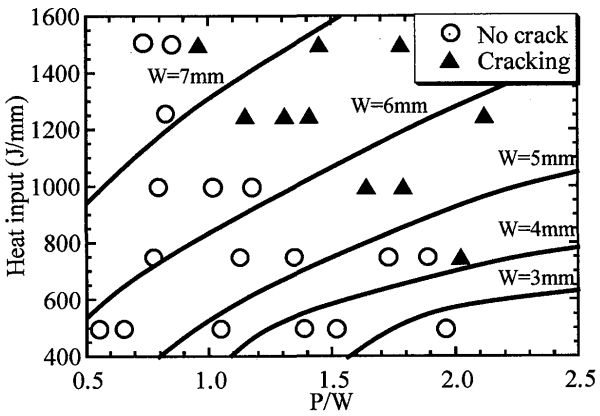

Fig.10 Influence of heat input and *P/W* on formation of pear-shaped bead cracking.

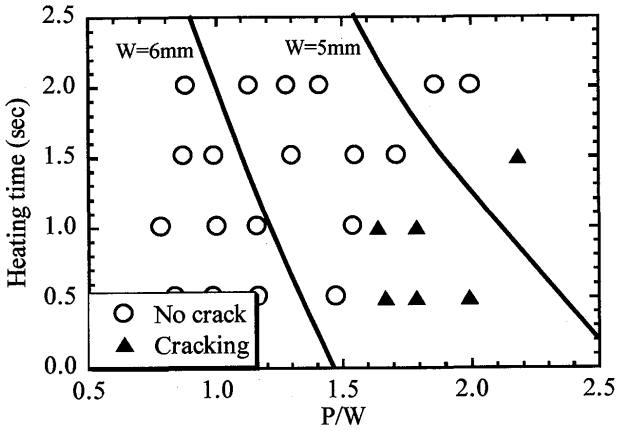

Fig.11 Influence of heating time and *P/W* on formation of pear-shaped bead cracking.

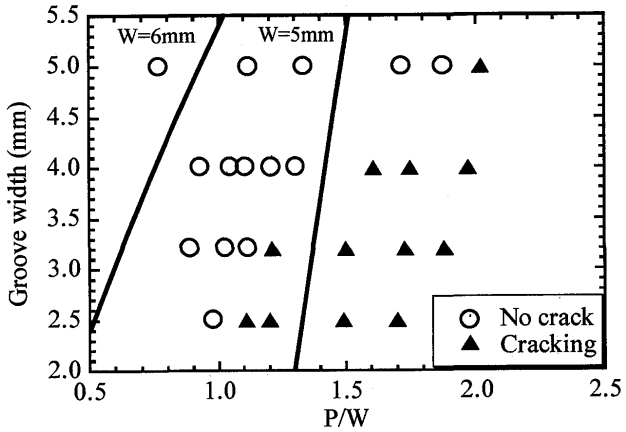

Fig.12 Influence of groove width and *P/W* on formation of pear-shaped bead cracking.

shows the maximum temperature distribution and the deformation after complete cooling. The area above 1450 °C represents the penetration where the metal is melted. In this case, the heat input is 1500 J/mm and the depth *P* and the width *W* of the penetration are 9.15 mm and 6.29 mm, respectively. The aspect ratio of penetration *P/W* is 1.45. As shown in Fig.9, pear-shaped bead cracking is formed in this case. The computed results are summarized in **Fig.10** with respect to the heat input *Q* and the aspect ratio *P/W*. The cases in which the crack is formed and not formed are represented by the solid triangles and the open circles, respectively. From this figure, it is seen that the cracking is more likely to occur when the heat input *Q* and the aspect ratio *P/W* are large. The contour lines drawn in the figure shows the penetration width *W*. Since the penetration width must be greater than the groove width to obtain a sound weld, the area where the penetration width is less than 5 mm must be disregarded.

3.2 Influence of welding speed

To examine the influence of the welding speed, serial computations were conducted by changing heating time and keeping the heat input constant at 1000 J/mm. The computed results are summarized in **Fig.11** in which the heating time and the *P/W* are taken as horizontal and vertical axes, respectively. It is seen that the cracking is likely to form when the welding speed is fast, in other words, when the heating time is short.

3.3 Influence of groove width

To clarify how the groove width influences the crack formation, serial computations were made for the four different values of the groove width, namely 2.5 mm, 3.2 mm, 4 mm and 5 mm and keeping the heat input as 750 J/mm. The computed results are summarized in **Fig.12**. It is clearly seen from the figure that the crack can be easily formed when the groove width is small. This may be explained by the fact that the restraint becomes larger and the area which solidifies at the last moment becomes deeper when the groove width is small.

3.4 Influence of solidification contraction

As it is shown in Fig.8, the volume change of the

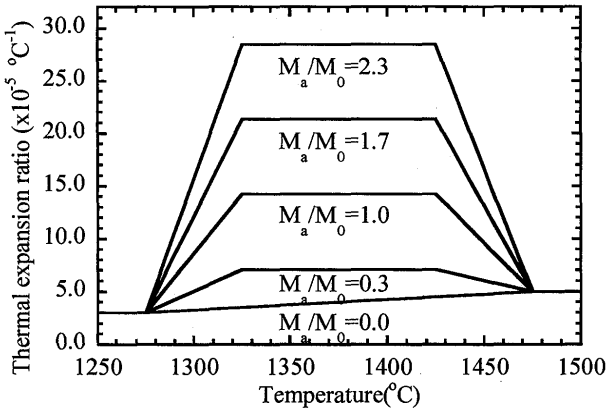

Fig.13 Temperature dependent thermal expansion ratio.

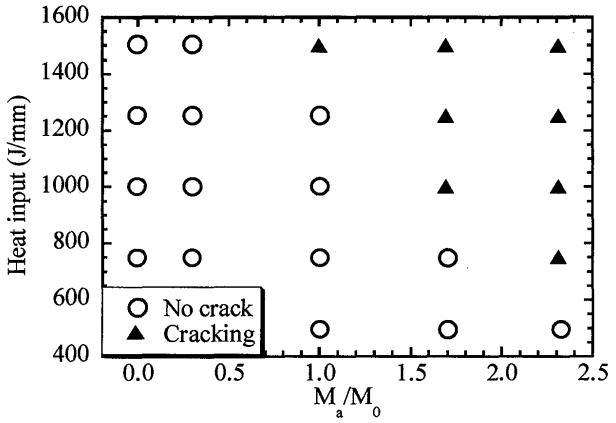

Fig.14 Influence of heat input and contraction during solidification on formation of pear-shaped bead cracking.

metal during the solidification is taken into account through the thermal expansion ratio in the *BTR*. To examine the influence of contraction during the solidification, the five cases with different values of volume change as shown in **Fig.13** are compared. Temperature range near the *BTR* is enlarged in Fig.13. The parameter M_α/M_0 is the ratio of the assumed volume change relative to the standard case. As seen from **Fig.14** which summarizes the computed results, cracking is promoted when the contraction during the solidification is large. This implies that the pear-shaped bead cracking is produced by the contraction during the solidification as in the case of castings.

When the groove is 2.5 mm, the pear-shaped bead cracking reaches to the surface in some cases such as shown in **Fig.15**. To closely examine this phenomenon, the computed results are plotted in **Fig.16** with respect to the heat input Q and the aspect ratio P/W, as in Fig.10, for cases in which the groove width is 5 mm. From the comparison between the two figures, it is seen that the crack can be formed in cases with relatively smaller values of P/W and the heat input when the groove width

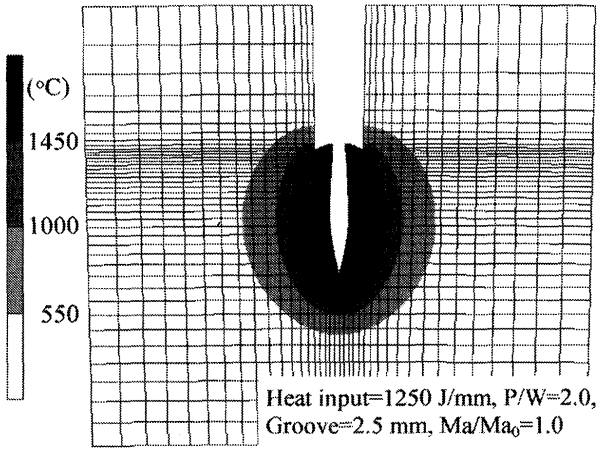

Fig.15 Maximum temperature distribution and with deformation with cracking.

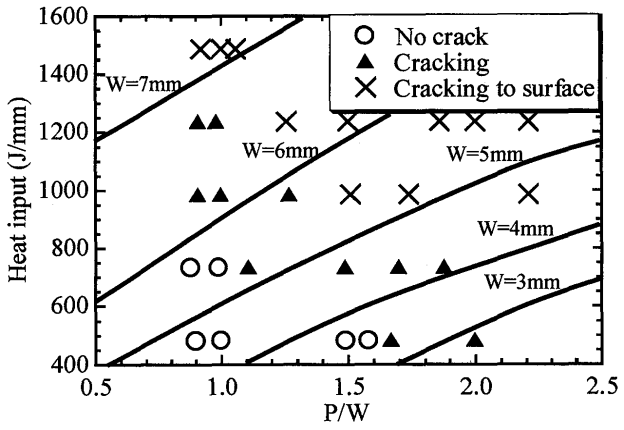

Fig.16 Influence of heat input and P/W on formation of pear-shaped bead cracking in cases where the groove width is 2.5 mm.

is 2.5 mm compared to those for 5 mm. It is also seen that the crack can reach the surface when both P/W and the heat input are larger than certain limits. In these cases, the crack is initiated near the center of the weld metal and extended to the surface. Through these computations, it is shown that types of crack which reach the surface and those that do not can both be simulated as observed in the experiment[1,2].

3.5 Influence of *BTR* width

The influence of the *BTR* width is examined by keeping other parameters constant. In these serial computations, the liquidus temperature is fixed at 1450 °C, and the solidus temperature is changed among five different values, namely 1200 °C, 1250 °C, 1300 °C, 1350 °C, and 1400 °C. **Figure 17** shows the computed results. From this figure, it is seen that the cracking tends to occur when the *BTR* width is larger, but the influence of the *BTR* width is not so significant compared with other parameters.

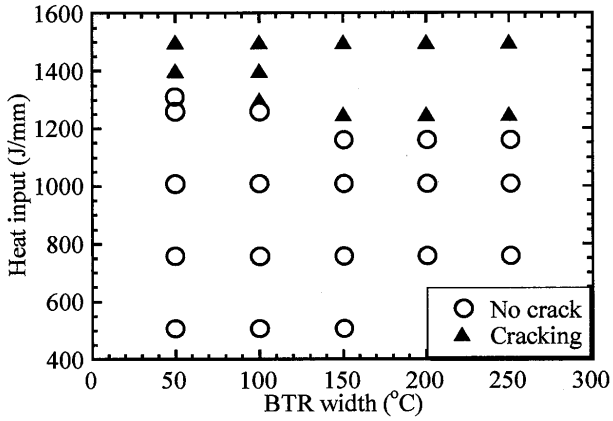

Fig.17 Influence of heat input and *BTR* width on formation of pear-shaped bead cracking.

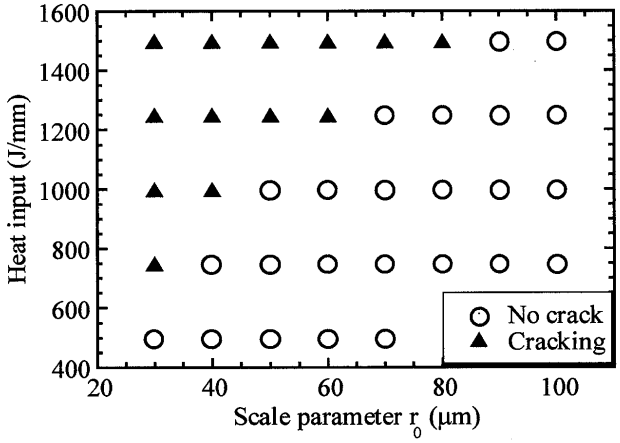

Fig.18 Influence of heat input and r_0 on formation of pear-shaped bead cracking.

3.6 Influence of scale parameter r_0

The influence of the scale parameter r_0 is examined through serial computations in which r_0 is changed from 30 μm to 100 μm. The computed results are summarized with respect to the scale parameter and the heat input in **Fig.18**. As clearly seen from the figure, the crack is likely to form when the scale parameter is small. This means that it is important to carefully select the value of the scale parameter for quantitative prediction.

3.7 How to achieve crack free weld with large aspect ratio

From the computed results shown in Figs. 10, 11 and 12, it is surmised that a sound crack free weld with large aspect ratio *P/W* can be achieved by choosing small heat input, slow welding speed and large groove width. However, these conditions may lead to low efficiency of welding. To achieve truly efficient welding, the welding conditions must be carefully selected considering three-dimensional effects if necessary.

Conclusions

The authors propose a temperature dependent interface element for the analysis of the pear-shaped bead cracking. Using the proposed method, serial computations were performed to clarify the influences of various factors on the formation of the cracking and the following conclusions were drawn.

(1) The two types of pear-shaped bead cracking, that reaching the surface and that which does not, can be simulated using the proposed method.

(2) Through the serial computations, it is found that the crack tends to be formed when the heat input, welding speed and the aspect ratio of the penetration are large. The cracking is also promoted when the groove width is small. These conclusions generally agree with experiments.

(3) Based on the investigation using the two dimensional model, it is found that small heat input, slow welding speed and large groove width is effective in achieving sound crack free welds with large aspect ratio *P/W*.

(4) The contraction during solidification is the essential cause of the pear-shaped bead cracking.

(5) When the *BTR* width and the scale parameter are small, the cracking is likely to occur. In particular, the scale parameter r_0 has a significant influence.

Acknowledgements

The authors would like to acknowledge that this research was conducted as a part of the joint research program between Kanazawa Institute of Technology and Joining and Welding Research Institute.

References

1) Y. Mori and I. Masumoto: "Considerations about the Forming of the Pear-Shaped Bead", *Jpn. Weld. Soc.*, Vol.48 (1979), No.12, pp.1041-1047. (in Japanese)

2) Y. Mori and I. Masumoto: "Considerations about the Forming of the Pear-Shaped Bead Crack", *Jpn. Weld. Soc.*, Vol.49 (1980), No.1, pp.19-23. (in Japanese)

3) T. Nakamura and K. Hiraoka: "Ultranarrow GMAW process with newly developed wire melting control system", *Science and Technology of Welding and Joining*, Vol.6 (2002), No.1, pp.355-362.

4) K. Nakata and F. Matsuda: "Evaluation of Ductility Characteristics and Cracking Susceptibility of Al Alloys during Welding", *Trans. of JWRI*, Vol.24 (1995), No.1, pp.83-94.

5) M. Shibahara, H. Serizawa and H. Murakawa: " FINITE ELEMENT METHOD FOR HOT CRACKING ANALYSIS USING TEMPERATURE DEPENDENT INTERFACE ELEMENT", *Mathe- matical Modelling of*

Weld Phenomena 5, (1999), pp.253-267.

6) M. Shibahara, H. Serizawa and H. Murakawa: "Finite Element Analysis Using Interface Element for Predicting Deformation during Butt Welding Considering Root Gap and Tack Welds", *TRANSACTIONS OF JWRI*, Vol.31 (2002), No.1, pp.63-70.